

## Development of microwave imaging reflectometry at NIFS

Y. Nagayama<sup>1)</sup>, D. Kuwahara<sup>2)</sup>, Z. B. Shi<sup>3)</sup>, S. Yamaguchi<sup>4)</sup>, T. Yoshinaga<sup>1)</sup>, S. Iio<sup>2)</sup>, S. Sugito<sup>1)</sup>,  
Y. Kogi<sup>5)</sup>, and A. Mase<sup>5)</sup>

<sup>1)</sup>National Institute for Fusion Science, 322-6 Oroshi-cho, Toki 509-5292, Japan

<sup>2)</sup>Tokyo Institute of Technology, 2-12-1 Ohokayama, Meguro-ku 152-8550, Japan

<sup>3)</sup>The Graduate University for Advanced Studies, 322-6 Oroshi-cho, Toki 509-5292, Japan

<sup>4)</sup>Kansai University, 3-3-35 Yamate-cho, Suita 564-8680, Japan

<sup>5)</sup>KASTEK, Kyushu University, 6-1 Kasuga Koen, Kasuga 816-8580, Japan

February 2, 2009

The Microwave Imaging Reflectometry (MIR) is under development at National Institute for Fusion Science (NIFS) in order to observe density fluctuations. The MIR makes a image of cutoff surface on the imaging detector array. The first MIR system, which is installed in the TPE-RX RFP device, uses the 20 GHz wave and the 4×4 plenary Yagi-Uda antenna array. The second MIR system, which is installed in the large helical device (LHD), uses the 60 GHz wave and the 8×5 horn antenna array. Those imaging detectors are newly invented in this research.

### 1 Introduction

The research object of the National Institute of Natural Sciences (NINS), to which the National Institute for Fusion Science (NIFS) belongs, is science of complex systems. Imaging, such as microscope and telescope, is a strong tool to investigate complex systems, and the NINS has started Imaging Science Project.

In terms of the illumination, imaging is divided by two: one is the "passive" imaging and another is the "active" imaging. In the case of the passive imaging, the observer uses only a imaging detector to take a picture with natural illuminations or self radiation from the object. In the case of the active imaging, the observer uses both a imaging detector and a illumination.

One of the most attractive imaging for the magnetically confined fusion plasma is the microwave with the following reasons: (1) The plasma radiates microwave as the electron cyclotron emission (ECE), of which intensity is proportional to the electron temperature; (2) The plasma reflects the microwave at the cutoff electron density. Since different frequencies of ECE or the reflection correspond to different locations, the cross-sectional image can be also observed [1]. As ECE is very sensitive to the variation of the electron temperature, the ECE imaging is very powerful tool to investigate MHD instabilities [2, 3]. As the microwave reflection at the cutoff surface is very sensitive to the variation of the electron density, the reflectometry is very powerful tool to investigate both MHD instabilities and electro-static instabilities [4]. Electro-static instabilities causes the variation of electron density.

The ECE imaging is a passive microwave imaging and the microwave imaging reflectometry (MIR) is an active microwave imaging, as shown in Fig. 1. The microwave

imaging system consists of a imaging optics, a microwave illumination system, a imaging detector array, a multi-channel frequency separator, DC circuits, and digitizers, as shown in Fig. 1. The frequency separator consists of bandpass filters and RF amplifiers. The frequency width of a bandpass filter for ECEI is wide. Since the ECE is a black-body radiation, the signal intensity of ECE is higher as the bandwidth is wider. The frequency width of a bandpass filter for MIR is narrow. Since the MIR signal is the reflection of the illuminated wave, the noise intensity of MIR is lower as the bandwidth is narrower. In order to reduce the bandwidth for MIR, the frequency difference between the illumination wave and the local wave should be well stabilized.

Despite of the usefulness of the microwave imaging, only one group has been successful to observe the plasma with microwave imaging in the world [6]. They obtain a 2-D cross-sectional image of the electron temperature with a 1-D imaging detector array and a frequency separator array [5, 6]. Their imaging detector uses dual-dipole antenna with a substrate lens. This antenna is attached with a long balun to transform the circuit from the antenna balanced circuit to the unbalanced antenna circuit. Since balun and antenna is on the same substrate, their detector array should be one dimensional.

One of key technologies of the microwave imaging is a imaging detector array. No 2-D imaging detector array has been used in the microwave imaging for plasma diagnostics yet. A multi-channel frequency separator is another issue. A microwave imaging system uses many imaging detector channels and tremendous number of frequency separator channels. For example, a 8 × 5 2-D imaging detector array has 40 channels. If each detector channel is connected to a frequency separator dividing 8 frequency channels, the total channel number is 480. Both the cost

author's e-mail: nagayama.yoshio@nifs.ac.jp

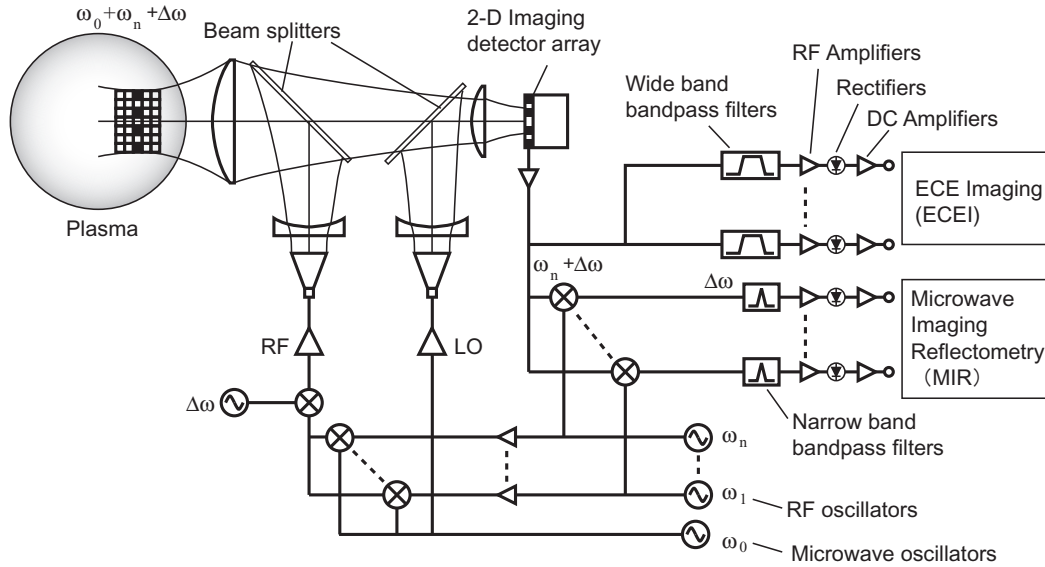


Fig. 1 Schematic view of microwave imaging system.

and the size should be very small to be installed. In the imaging science project, a  $8 \times 5$  60 GHz 2-D imaging detector arrays [8] and a 8 channel frequency separator [9] have been developed.

The microwave imaging is under development as a NINS imaging science project at NIFS. The prototype of the MIR was installed in 2006 [?, ?]. The prototype MIR has 3 frequencies (53, 66, 69 GHz) for illuminating wave and 3 horn antennas to receive reflection wave. A  $4 \times 4$  20 GHz 2-D imaging detector array using planer Yagi-Uda antenna has been developed. The first MIR system was developed and installed in the TPE-RX reversed field pinch device at the National Institute of Advanced Industrial Science and Technology (AIST) in 2007 [12, 13]. This system uses the 20 GHz 2-D imaging detector array. The second MIR system has been developed to be installed in the LHD at NIFS. This system uses the 60 GHz 2-D imaging detector array. This paper presents those MIR systems developed at NIFS.

## 2 Proto type MIR System in LHD

Figure 2 shows a schematic diagram of the prototype MIR system in LHD. The illumination wave (RF) is generated by 3 high power (0.5 W) IMPATT oscillators, whose frequencies are 53, 66 and 69 GHz, respectively. These oscillators used to be installed 5 m far from LHD. However, the operation of the IMPATT oscillators was interfered by the leakage of the magnetic field. Actually, the output power of the IMPATT oscillators reduces as the magnetic field increases, and finally no output power are observed. After enclosing in 5 mm thick soft-iron shield case, the power was dropped by 30 %. Therefore the microwave sources are installed 15 m far from LHD and the microwave is transferred using oversized rectangular

waveguides (X-band, WR-90) and 90 degree H bends. By using optical system, the illumination wave radiated from a horn antenna (WR-15) is formed to a parallel beam with a diameter of 20 cm at the reflection layer in the plasma. The illumination wave is reflected by the three cutoff layers, which are determined by the local density and the magnetic field in the case of X-mode reflection.

The primary imaging mirror (M1) is installed in the LHD vacuum vessel. This is an elliptic concave mirror with the size of  $43 \times 50$  cm and the focal length of 106.5 cm. The distance between the mirror M1 and plasma is 210 cm. The mirror M1 is remotely manipulated by the use of ultrasonic motors (USMs). Since the LHD plasma is twisted, toroidal and poloidal angles of the main mirror should be controlled within 1 degree in order to obtain reflection from plasma.

The reflected wave is accumulated by the primary imaging mirror. ECE and the reflected wave are separated by a dichroic plate (DP), which is a high pass filter with a sharp cut-off frequency of 70 GHz. This dichroic plate is an 8 mm thick aluminum alloy plate with many circular holes. The diameter of each hole is 2.5 mm and they are separated by 2.8 mm. The hole has the angle of 45 degree to the plate so that ECE wave more than 70 GHz efficiently passes through the dichroic plate.

The reflected beam and the illumination beam are separated by the beam splitter (BS), which is a 3 mm thick Plexiglas plate. The reflected illumination beam by BS and the transmitting illumination beam through DP are absorbed by microwave absorbing forms (ECCOSORB CV-3) in order to reduce background noise. Because of microwave absorbers and beam separation, the leakage of the illumination wave to the receiver is significantly reduced, so that the background level in the signal is drastically reduced.

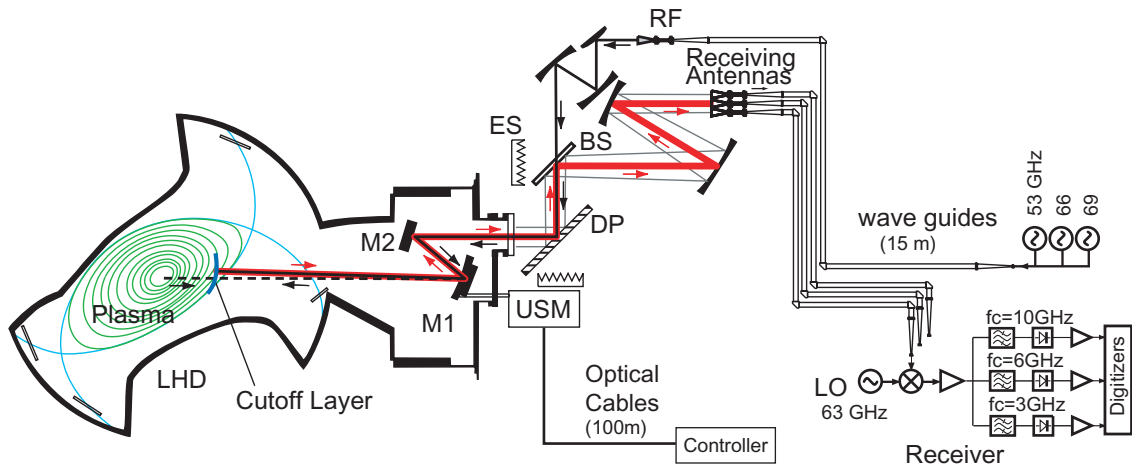


Fig. 2 Schematic view of the prototype of MIR system in LHD. M1: Adjustable concave mirror, M2: Plane mirror, DP: Dichroic plate (70GHz), BS: Beam splitter, US: Ultrasonic motor, ES: ECCOSORB CV3.

The plasma image is formed on the front end of receiving horn antenna (WR-15) array by the mirror optics. The pair of antennas is separated by 8.4 cm in the poloidal direction, and another pair by 10.7 cm in the toroidal direction on the cutoff layer. Received reflection wave is transmitted to the heterodyne receiver with oversized waveguides (X-band). In the heterodyne receiver, reflected wave is mixed with the wave from local oscillator (LO) with the frequency of 63 GHz to make intermediate frequency (IF) signals. IF signals selected by band-pass-filters with the bandwidth of 10 % of the central frequency are amplified by modular RF amplifiers. Finally they are rectified by Schottky barrier diodes, amplified by DC amplifiers and digitized by PXI digitizer modules.

By using this system, the edge harmonic oscillations are observed [14].

### 3 MIR System in TPE-RX

TPE-RX is a large reversed field pinch (RFP) in the world. The major radius is 172 cm and the minor radius is 45 cm. With 20 GHz reflectometry, of which cutoff density is  $0.5 \times 10^{19} \text{m}^{-3}$ , the density fluctuation can be observed when  $n_{av} > 0.4 \times 10^{19} \text{m}^{-3}$ . In the typical TPE-RX plasma, the cutoff frequency near the field reversal surface, where the toroidal field changes the direction, is about 20 GHz. Therefore, we use 20 GHz for MIR in TPE-RX.

Figure 3 shows a schematic diagram of the MIR system in TPE-RX. The quartz window of the TPE-RX viewing port is located at  $r = 67$  cm, the illumination wave (RF) can pass through the window. The primary mirror ( $M_1$ ), which is an elliptic concave mirror with the size of  $40 \times 43$  cm, makes a parallel illumination beam in the plasma. The reflected wave is collected by  $M_1$  and is separated from the illumination beam by the first beam splitter ( $BS_1$ ). The local oscillation (LO) wave and the reflected wave is mixed

with the second beam splitter ( $BS_2$ ). These beam splitters are 3 mm thick Plexiglas plates. The RF wave reflected by  $BS_1$  and the LO wave passing through  $BS_2$  are absorbed by a microwave absorber in order to reduce background noise. An image of the reflection layer is made on the 2-D mixer array by the Teflon lens ( $L_1$ ).

In this experiment, two types of 2-D mixer array are used. One is a 2-D array of coax to waveguide adapters with diodes. The waveguide is for the frequency bandwidth of 18–26.5 GHz and has the inner size of  $1.07 \times 0.43$  cm. These adapters are separated by 2.24 cm. Another is a 2-D planar Yagi-Uda antenna array on a Teflon printed circuit board (PCB) with the thickness of 0.254 mm. In the 2-D Yagi-Uda antenna array, four elements are set on a PCB with a distance of 12 mm, and 4 PCBs are stacked with a distance of 15 mm. Each element consists of a planar Yagi-Uda antenna, a balun, a beam lead type Schottky barrier diode (SBD) and an IF amplifier. In this system, a tapered balun is used, and this is different from the original planar Yagi-Uda antenna system. On the design of antenna system, a computer code for electro-magnetic field is employed. This Yagi-Uda antenna has 3 guiding elements, a pair of dipole and a reflector element. The IF amplifier consists of surface acoustic wave (SAW) bandpass filters and RF amplifiers. Also the mixer element has two voltage regulators for the power supply of amplifier and the DC bias of SBD. The signal output is a MMCX straight PCB jack connector. The 2-D mixer array is contained in a shield box that has 16 SMA connectors for the signal output. The MMCX and SMA are connected with a coaxial cable inside the shield box.

The LO wave ( $\omega + \omega_1$ ) is made by mixing the RF wave ( $\omega$ : 20 GHz) and the lower frequency wave generated by a crystal oscillator ( $\omega_1$ : 110 MHz) at an up-converter. Lenses  $L_1$  and  $L_2$  make a spot of LO wave with the diameter of 10 cm on the 2-D mixer array. By mixing the reflected wave with the frequency of  $\omega$  and the LO wave,

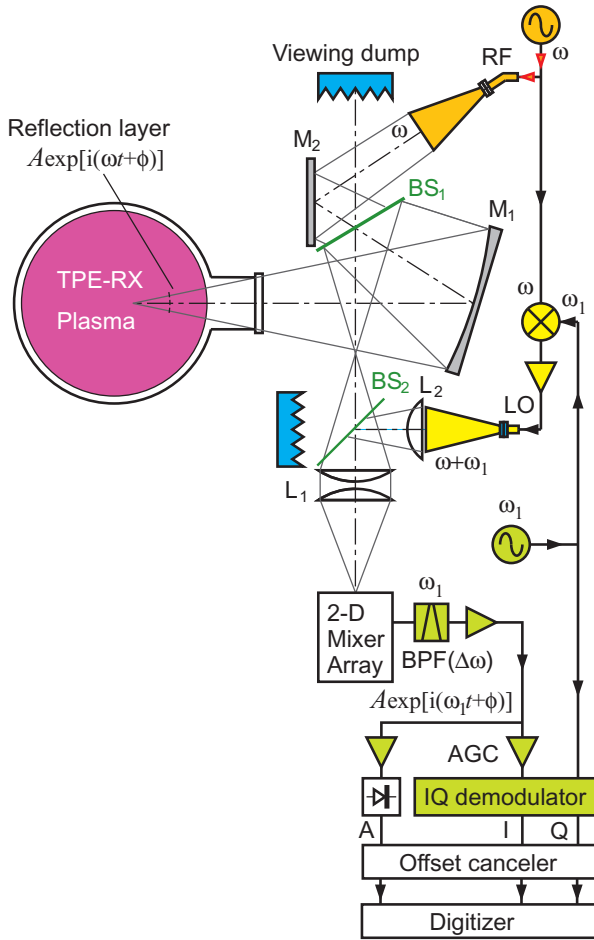


Fig. 3 Schematic view of MIR system in TPE-RX.

the 2-D mixer array makes IF signal with the frequency of  $\omega_1$ . Since the IF frequency  $\omega_1$  is well stabilized, the noise can be significantly reduced because the bandwidth of the IF amplifier is narrow (4 MHz).

The reflective wave contains the amplitude  $A$  and the phase  $\phi$ , as,  $A \exp[i(\omega t + \phi)]$ , where the amplitude  $A$  and the phase  $\phi$  is generated by a density fluctuation in the plasma. The phase  $\phi$  indicates the vibration motion of the reflection layer. The IF signal also contains the amplitude and the phase, as  $A \exp[i(\omega_1 t + \phi)]$ . The amplitude is obtained by rectifying the IF signal with microwave monolithic integrated circuit (MMIC). The phase is obtained by comparing the IF frequency and the signal by the IQ demodulator. I and Q signals correspond to  $\cos\phi$  and  $\sin\phi$ , respectively.

Due to RF noise, the rectified RF signal contains large offset. This offset is removed by an offset canceler, which consists of a differential amplifier and a sample-hold circuit. The sample-hold circuit works as follows: a digitizer samples the MIR data at  $t = 0$  and hold it in a digital memory, then an digital to analog converter makes analog output. By using the differential amplifier the offset that is the analog output of the sample-hold circuit is removed from the MIR signal.

By using this system, MHD turbulences in RFP plas-

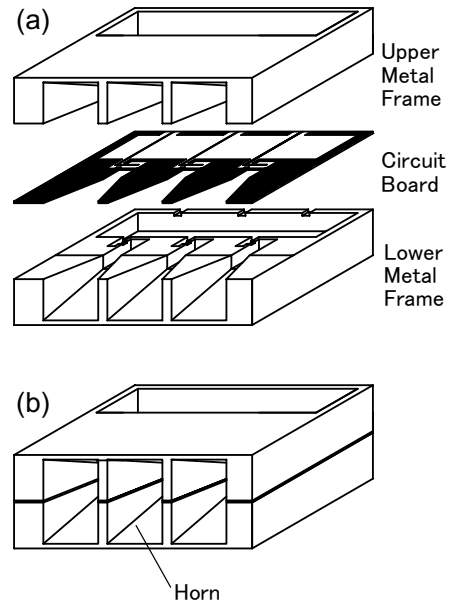


Fig. 5 Schematic view of an assembly of horn antenna array. (a) Parts; (b) Completed form.

mas are observed [13].

#### 4 2-D MIR System in LHD

Figure 4 shows a schematic diagram of the 2-D MIR system in LHD. The optical system is almost the same as the prototype MIR system. The difference is optics for the LO wave and thickness of the beam splitters. Since the 2-D detector contains mixers, the LO wave illuminate the 2-D detector by using a beam splitter.

The illumination wave (RF) is the mixture of the LO wave (frequency:  $\omega_0$ ) and the IF frequency (frequency:  $\omega_L$ ) with an up-converter. Due to small leak of original frequency, the RF wave includes a small amount of  $\omega_0$  and a major part of  $\omega_0 + \omega_L$ . If this wave is used as LO wave, the detector generates an IF signal of  $\omega_L$  without reflection. Since the reflection is much weaker than the illumination, a strong LO wave is required to make an IF signal. In this case, the IF frequency is 110 MHz, which is generated by a crystal oscillator.

The local oscillation (LO) for the heterodyne detection is made by up-converting the VCO signal and a crystal oscillator's signal, to generate an intermediate frequency (IF) of 110 MHz. We are also developing band-pass filter-banks, IF amplifiers and I-Q demodulators. The band-pass filter-bank uses the microwave strip line technology. The I-Q demodulator is a phase detector of reflected signals.

A schematic view of an assembly of the imaging detector array is shown in Fig. 5. This detector array is made of 3 major parts, such as the upper metal frame, a circuit board and a lower metal frame, as shown in Fig. 5(a). The upper and lower metal frame are made of aluminum alloy,

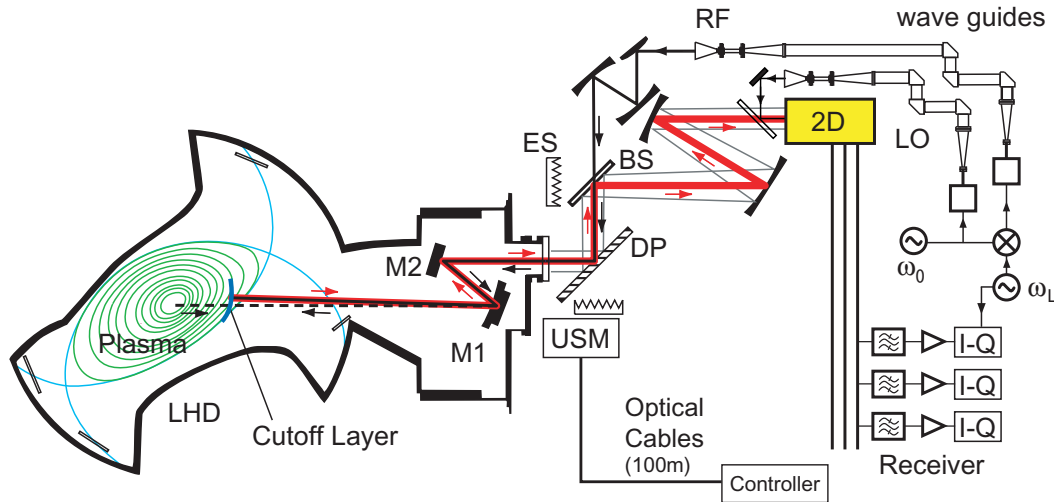


Fig. 4 Schematic view of the 2-D MIR system in LHD.

and horn shape and waveguide slots are made by electrical discharge machining. By attaching these slots, a horn antenna is formed, as shown in Fig. 5(b). In the upper structure, another slot is formed for passing the microstrip-line. On the circuit board the mixer diode, filters and RF amplifiers are mounted. The circuit is produced by the micro-strip-line technology. The horn antenna receives both RF and LO waves and the mixer generates an intermediate frequency (IF) signal. The mixer bias is supplied from a DC power supply through an inductor, and the bias current is optimized. The IF amplifiers is low-cost GaAs microwave monolithic ICs with the frequency range of DC to 10 GHz and the 13 dB. Its power is supplied from RF output through the choke inductor and the current limit resistor. The DC-blocking capacitors are needed after the output of the amplifier. By stacking this 1-D array, a 2-D array (5 in toroidal and 8 in toroidal directions) is formed.

The frequency response the reflectivity of different 90 degree beam splitters is shown in Fig. 6. Here, a mylar sheet (thickness: 0.2 mm), plane acrylic glasses (thickness: 1 mm and 2 mm) and a high refractive index board (thickness: 2.54 mm) are tested. The amount of reflection differs as the polarization differs. Despite of the polarization, a transparent frequency window is observed in thick beam splitters. In the case of 90 degree beam splitter with the thickness of 2 mm, the transparent frequency is 47.2 GHz, of which wavelength is 6.35 mm in vacuum. In the case of 180 degree beam splitter with the thickness of 2 mm, the transparent frequency is 42.2 GHz, of which wavelength is 7.1 mm in vacuum. An acrylic glass with the thickness of 1 mm is used as a beam splitter.

The I/Q demodulator is under development to measure the phase difference between the probe wave and the reflected wave. It outputs the three components of  $\cos \phi$ ,  $\sin \phi$  and the reflected power of the 110 MHz intermediate frequency ( $\phi$  is the phase difference between the probe wave and reflected wave). The I/Q demodulator consists

of a low-price quadrature demodulator IC-chip (the unit price is about 15 dollars) with the auto-gain control function. The output frequency range is DC - 1 MHz, which is higher than the typical frequency range of 1 - 500 kHz of the density fluctuation in LHD. The input power is automatically adjustable between -80 and -30 dBm. The low-cost version of the I/Q demodulator with the unit price of less than 100 dollars is now under development in NIFS.

## 5 Conclusion

Microwave Imaging Reflectometry is under development in order to obtain the 2-D/3-D image of the electron density fluctuation in the TPE-RX RFP device and in the Large Helical Device. The MIR becomes a powerful tool to investigate the micro-turbulence and the magneto-hydrodynamic instability in the magnetically confined plasma. By using the microstrip line technology three key devices are under development for the LHD plasma experiment and the industrial applications. The 2-D detector array is developed by stacking of 1-D detector arrays of the planar Yagi-Uda antenna for 20 GHz and the horn antenna for 60 GHz. The intermediate frequency receiver with the bandpass filter and the RF amplifiers is installed on the same board of the antenna array. The I/Q demodulator is under development for the multi-channel phase measurement of the phase difference between the probe wave and the reflected wave. These devices enable the multi-channel microwave imaging system for 2-D/3-D observation in the plasma diagnostics.

**Acknowledgement** This works is supported by National Institute for Fusion Science (Grant No. NIFS08ULPP525) and by National Institute of Natural Sciences (Grant No. NIFS08KEIN0021).

- [1] Y. Nagayama, *Rev. Sci. Instrum.* **65**, 3417 (1994).
- [2] Y. Nagayama, et al., *Phys. Plasmas* **3**, 2631 (1996).



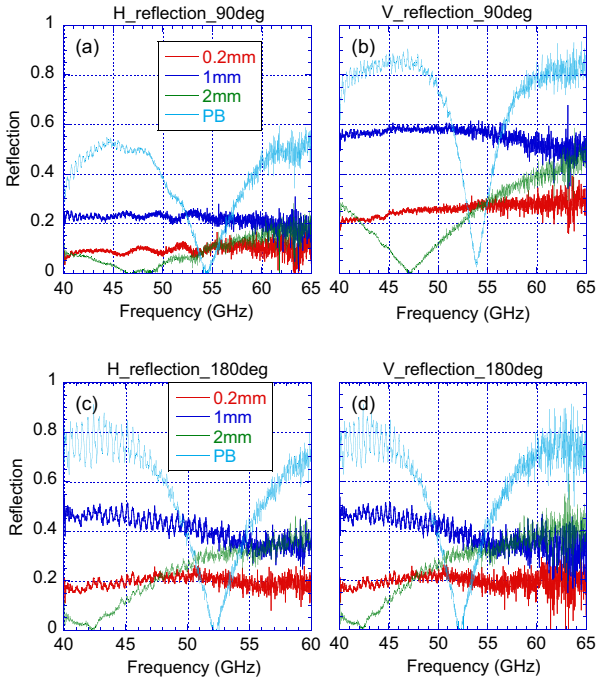


Fig. 6 The reflectivity of 90 degree beam splitters. (a) The polarization is perpendicular to the beam splitter. (b) The polarization is parallel to the beam splitter. Numbers indicates thickness of acrylic glass of beam splitter. PB is a high reflective index board with the thickness of 2.54 mm.

[3] Y. Nagayama, et al., *Phys. Plasmas* **3**, 1647 (1996).  
 [4] E. Mazzucato, *Rev. Sci. Instrum.* **69**, 2201(1998).  
 [5] C.W. Domier, et al., *Rev. Sci. Instrum.* **77**, 10E924 (2006).  
 [6] H. Park, et al., *Phys. Rev. Letters*, **96**, 195003 (2006).  
 [7] Z. Shen, et al. *Plasma Fus. Res.*, **2**, S1019 (2007).  
 [8] D. Kuwahara, et al., "Development of 2-D Antenna Array for Microwave Imaging Reflectometry in LHD", *Plasma Fusion Res. JPFR Series* (to be published in 2009).  
 [9] Y. Kogi, et al., *Rev. Sci. Instrum.* **79**, 10F115 (2008).  
 [10] S. Yamaguchi, et al., *Rev. Sci. Instrum.* **77**, 10E930 (2006).  
 [11] S. Yamaguchi, et al., *Plasma Fusion Res.* **2**, S1038 (2007).  
 [12] Y. Nagayama, et al., *Plasma Fusion Res.* **3**, 053 (2008).  
 [13] Z.B. Shi, et al., *Plasma Fusion Res.* **3**, S1045 (2008).  
 [14] S. Yamaguchi, et al., "Observation of MHD mode with higher harmonics in the edge plasma region in the Large Helical Device", (submitted to *Phys. Plasmas*).